First-principles investigation of the electronic and Li-ion diffusion properties of LiFePO4 by sulfur surface modification

Guigui Xu, Kehua Zhong, Jian-Min Zhang, and Zhigao Huang

Citation: Journal of Applied Physics **116**, 063703 (2014); doi: 10.1063/1.4892018
View online: http://dx.doi.org/10.1063/1.4892018
View Table of Contents: http://scitation.aip.org/content/aip/journal/jap/116/6?ver=pdfcov
Published by the AIP Publishing

First-principles investigation of the electronic and Li-ion diffusion properties of $LiFePO_4$ by sulfur surface modification

Guigui Xu,[1,2,3,a] Kehua Zhong,[2,3] Jian-Min Zhang,[2,3] and Zhigao Huang[2,3,a]
[1]*Concord University College Fujian Normal University, Fuzhou 350117, China*
[2]*College of Physics and Energy, Fujian Normal University, Fuzhou 350117, China*
[3]*Fujian Provincial Key Laboratory of Quantum Manipulation and New Energy Materials, Fuzhou 350117, China*

(Received 19 June 2014; accepted 22 July 2014; published online 12 August 2014)

We present a first-principles calculation for the electronic and Li-ion diffusion properties of the $LiFePO_4$ (010) surface modified by sulfur. The calculated formation energy indicates that the sulfur adsorption on the (010) surface of the $LiFePO_4$ is energetically favored. Sulfur is found to form Fe-S bond with iron. A much narrower band gap (0.67 eV) of the sulfur surface-modified $LiFePO_4$ [S-$LiFePO_4$ (010)] is obtained, indicating the better electronic conductive properties. By the nudged elastic band method, our calculations show that the activation energy of Li ions diffusion along the one-dimensional channel on the surface can be effectively reduced by sulfur surface modification. In addition, the surface diffusion coefficient of S-$LiFePO_4$ (010) is estimated to be about 10^{-11} (cm^2/s) at room temperature, which implies that sulfur modification will give rise to a higher Li ion carrier mobility and enhanced electrochemical performance. © *2014 AIP Publishing LLC*.
[http://dx.doi.org/10.1063/1.4892018]

I. INTRODUCTION

$LiFePO_4$ is a promising new-generation cathode material for Li rechargeable batteries due to its high energy density, good thermal stability, low cost, and environmental friendliness.[1–3] However, poor intrinsic electronic and ionic conductivity hamper its extensive application in high-rate lithium ion batteries.[4,5] To overcome this limitation, various approaches of synthesis and material modification have been devoted to enhancing the electronic and ionic conduction for $LiFePO_4$ in recent years.[6–11] Surface modification is well-known as an effective way to improve the rate performance of $LiFePO_4$ cathode. For instance, early studied results indicated that, with carbon coating, Li ions can be reversibly extracted out of $LiFePO_4$, giving rise to a capacity as high as 160 mAh/g that is close to the theoretical capacity of 170 mAh/g.[12] Recently, Lin *et al.*[11] revealed that the Sn-coated $LiFePO_4$/C exhibits higher capacity, better cyclability and higher rate capability in a wide operation temperature range. Park *et al.*[13] found that anion surface modification of $LiFePO_4$ can greatly improve the charge transfer kinetics and the charge/discharge performance owing to the stronger Li^+ binding on the surface sites in the presence of nitrogen or sulfur on the surface of $LiFePO_4$. However, despite the observed electrochemical performance improvement of the surface-modified $LiFePO_4$, in-depth theoretical understanding about the origin of the improvement in terms of an electronic and ionic contribution and what causes these differences have not been clearly achieved yet.

Previous reports gave theoretical[14,15] and experimental[16] evidence of one-dimensional lithium ion diffusion pathway along [010] direction in $LiFePO_4$. In addition, based on $LiFePO_4$ surface simulation using first-principles calculations, Wang *et al.*[17] found that the (010) surface is prominent in the crystal morphology. Moreover, plate-like $LiFePO_4$ nanocrystallites with preferential growth of the (010) lattice plane have been successfully prepared in experiment.[18] Therefore, in this work, we would like to focus our study on the (010) surface of the $LiFePO_4$ since it is normal to the favored [010] diffusion pathway, which facilitates Li access to all the particle volume. Recently, Dathar *et al.*[19] reported that surface diffusion has the higher activation energy than bulk diffusion, which could contribute to slow kinetics in nanostructured $LiFePO_4$ cathode. Therefore, efforts to reduce the surface diffusion barrier are essential in order to optimize rate performance. In this paper, we report a method to enhance the electronic and ionic conduction by the introduction of sulfur to the $LiFePO_4$ (010) surface. Here, we mainly investigate the electronic and Li-ion diffusion properties of the sulfur-modified $LiFePO_4$ (010) surface [S-$LiFePO_4$ (010)] using DFT+U method and to explore the effects of the surface modification on the rate performance. Additionally, the framework of density functional theory (DFT) was employed together with the climbing image nudged elastic band method (NEB) to gain insights about the lithium migration pathways as well as the diffusion barriers.

II. METHOD

Calculations were performed based on density functional theory in the generalized gradient approximation (GGA)[20] and the projector-augmented wave (PAW) method[21] with a plane-wave basis was employed, as implemented in the Vienna *ab initio* simulation package (VASP) code.[22] For all calculations, an energy cutoff of 500 eV was used. Calculations for bulk olivine-type $LiFePO_4$ were performed using a $3 \times 5 \times 6$ Monkhorst-Pack *k*-point mesh with Γ-centered. For a calculation of the electronic density of

[a]Authors to whom correspondence should be addressed. Electronic addresses: xuguigui082@126.com and zghuang@fjnu.edu.cn.

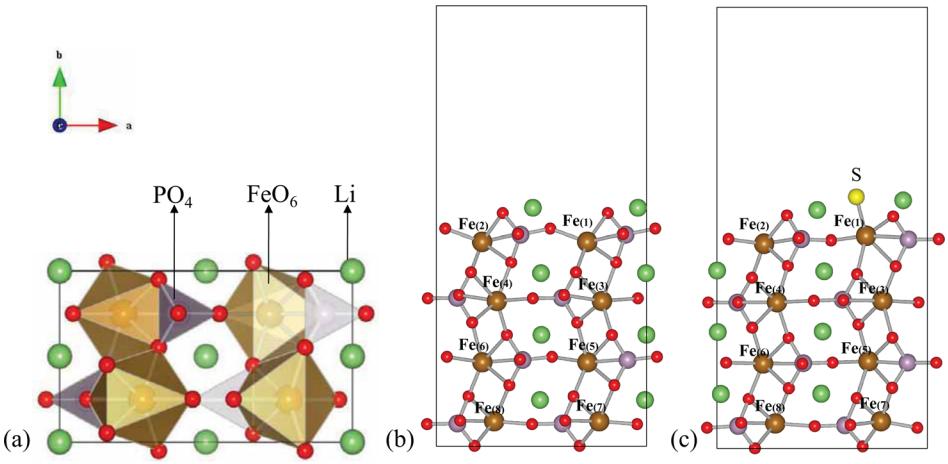

FIG. 1. (a) The crystal structure of $LiFePO_4$. The relaxed surface structures of (b) $LiFePO_4$ (010) surface and (c) $LiFePO_4$ (010) surface adsorbed with S atom.

states, a denser *k*-mesh of $6 \times 10 \times 12$ was used. The on-site Coulomb interaction of Fe-3*d* electrons was described by a Hubbard U introduced by Dudarev *et al.*[23] A U_{eff} (U-J) value of 4.3 eV was chosen based on the average values for Fe^{2+} ($U_{eff} = 3.7$ eV in $LiFePO_4$) and Fe^{3+} ($U_{eff} = 4.9$ eV in $FePO_4$) calculated by Zhou *et al.*[24] For $LiFePO_4$ olivine system, the GGA + U level of theory has been used to accurately calculate the electronic structures and to guarantee that the excess holes or electrons are properly localized.[25] A ferromagnetic spin configuration was set for the Fe ions. Geometry optimizations were considered converged when the force on each atom was less than 0.01 eV/Å.

The initial unrelaxed (010) surface structure was carved out of the fully relaxed bulk $LiFePO_4$ crystal. The surface calculations were performed on a slab model.[26] Convergence test with respect to the slab thickness was carried out with a 1×1 surface unit cell. It was found that a slab of 12.1 Å is sufficient to get a converged surface energy for the low energy (010) surface termination. Considering the efficiency of the computations, a smaller 1×1 surface supercell was used for the study in this work. Thus, a supercell was constructed of 1×1 unit cell on the *ac* plane, and 12.1 Å in the *b*-direction, with 10 Å vacuum separating the periodic slabs. The Brillouin-zone integration was performed within the Monkhorst-Pack scheme using *k* meshes of $(3 \times 6 \times 1)$ and $(6 \times 12 \times 1)$ for the geometry relaxation and calculation of the electronic density of states, respectively.

Minimum energy pathway (MEP) and the activation energy for Li diffusion along the [010] direction were calculated with the climbing-image nudged elastic band (NEB) method.[27] Supercells containing $1 \times 2 \times 1$ unit cells were used to determine energy barriers for diffusion. Five intermediate images are constructed to interpolate the initial and final states along the Li diffusion path. In the calculation of the activation energy, all images and other ions in the supercell were allowed to relax to its equilibrium position, while the lattice parameters were held fixed.

III. RESULTS AND DISCUSSION

A. Structure models

Olivine-type $LiFePO_4$ has an orthorhombic crystal with the space group *Pnma* and the unit cell accommodates four $LiFePO_4$ formula-units, as shown in Fig. 1(a). The structure framework consists of FeO_6 octahedra and PO_4 tetrahedra with Li ion locating at the one-dimensional channel along [010] direction (*b* axis). The lattice parameter of the relaxed bulk $LiFePO_4$ structure is $a = 10.427$ Å, $b = 6.057$ Å, and $c = 4.743$ Å, respectively, in good agreement with the experimental values[28] and the other calculated results.[29] The initial,

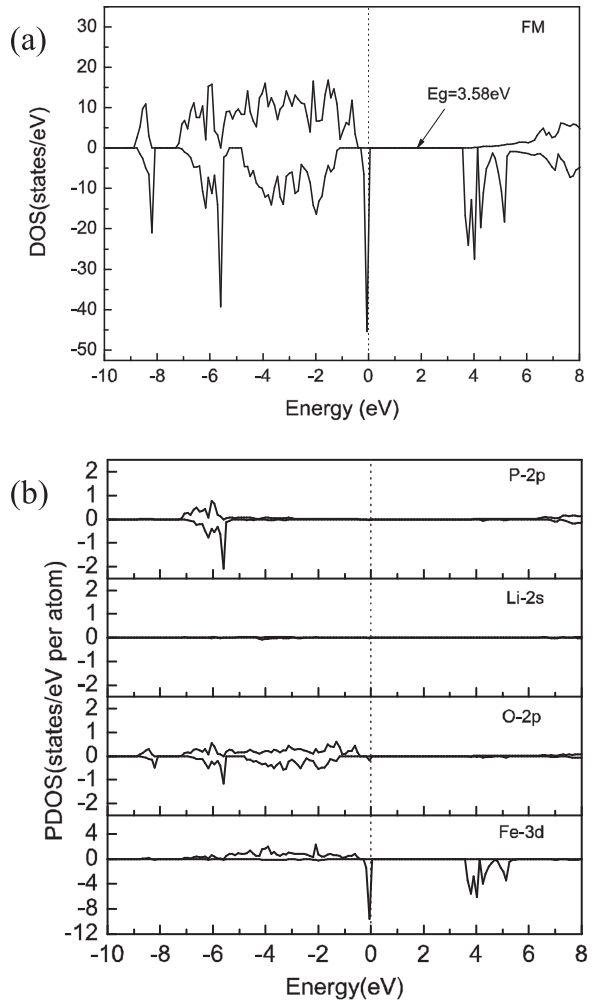

FIG. 2. (a) Total density of states (DOS) of bulk $LiFePO_4$. (b) Partial density of states (PDOS) of Fe-3*d*, O-2*p*, Li-2*s*, and P-2*p* in bulk $LiFePO_4$. The Fermi level is set to be zero.

unrelaxed (010) surface structure was carved out from the fully relaxed bulk crystal. The low energy (010) surface termination in the [010] direction cuts through the LiO_6 octahedra but only cuts the top of the FeO_6 octahedra, leaving threefold Li and fivefold Fe exposed on the surface. The relaxed surface structure of the low energy (010) surface is shown in Fig. 1(b). To test the stability of the surface structure, we calculated the surface energy. The surface energy is defined by[17]

$$\gamma = (E_S - nE_b)/2S, \tag{1}$$

where E_b is the total energy per formula unit of bulk $LiFePO_4$, E_s is the total energy of the given supercell containing n formula units of $LiFePO_4$, and S is the base area of the supercell. The calculated surface energy is 0.66 J/m^2, consistent with the value 0.64 J/m^2 reported by Wang *et al.*[17]

The (010) surface adsorbed with S atom after relaxation is displayed in Fig. 1(c). The fractional coordinates of S atom is (0.662, 0.570, 0.230), which is very close to the position of $Fe_{(1)}$ (0.709, 0.482, 0.021) in surface-terminated sites. The S–$Fe_{(1)}$ bond length is 2.216 Å. The bond lengths of S–Li and S–O are 2.369 Å and 3.179 Å, respectively. The covalent interactions of S-Li and S-O are weaker due to the relatively longer bond length. Sulfur induces a dramatic geometric distortion to the surface, and the PO_4 surface groups are rotated, as seen in Fig. 1(c). To characterize the stability of the surface adsorption structure, we calculated the surface adsorption energy. Surface adsorption energy is defined as follows:[30]

$$\Delta E_a = E_{S\_on\_(010)} - E_{(010)} - E_S, \tag{2}$$

where $E_{S\_on\_(010)}$, $E_{(010)}$, E_S represent the DFT total energies of the S-$LiFePO_4$ (010), $LiFePO_4$ (010), and isolated S atom, respectively. The calculated surface adsorption energy is −3.40 eV. A negative value of the surface adsorption energy indicates S adsorption on the $LiFePO_4$ (010) surface is energetically favorable.

B. Electronic structure

The electronic structures are studied in this section. Figs. 2(a) and 2(b) show the total electronic density of states (DOS) and partial density of states (PDOS) of bulk $LiFePO_4$ in ferromagnetic (FM) spin configuration. From Fig. 2(a), it is found that bulk $LiFePO_4$ is a semiconductor with energy gap of 3.58 eV according to the GGA + U calculation, in agreement with the previously reported value (of 3.58 eV) by Hoang *et al.*[31] and the experimental results (about 3.8–4.0 eV).[32,33] The large band gap prevents the intrinsic generation of an electron or hole, so pure bulk $LiFePO_4$ shows poor electron conductivity. Although some recent theoretical studies have

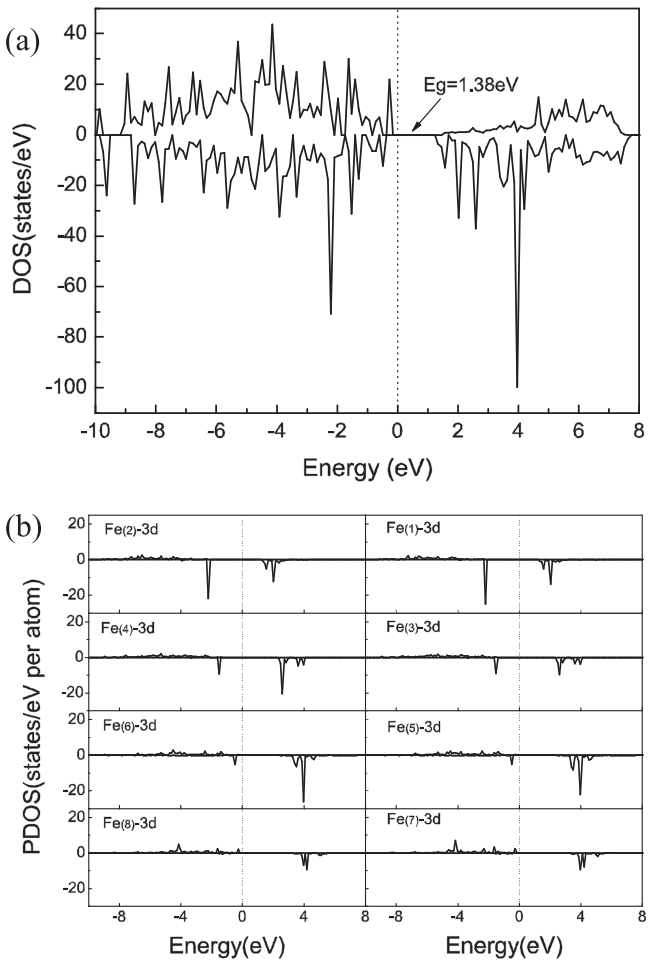

FIG. 3. (a) Total DOS of pure $LiFePO_4$ (010) surface. (b) The PDOS of Fe atoms at different positions in pure $LiFePO_4$ (010) surface. The Fermi level is set to be zero.

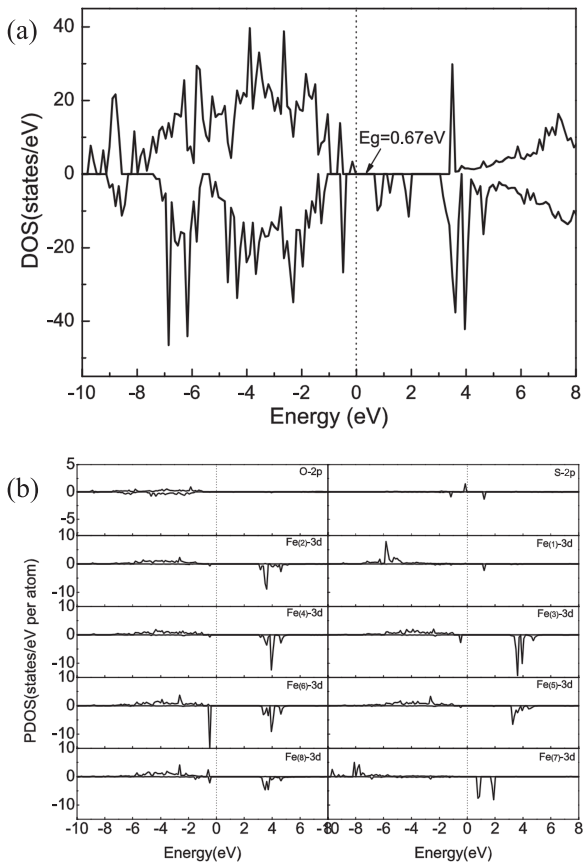

FIG. 4. (a) Total DOS of $LiFePO_4$ (010) surface adsorbed with S. (b) The PDOS of $LiFePO_4$ (010) surface adsorbed with S. The Fermi level is set to be zero.

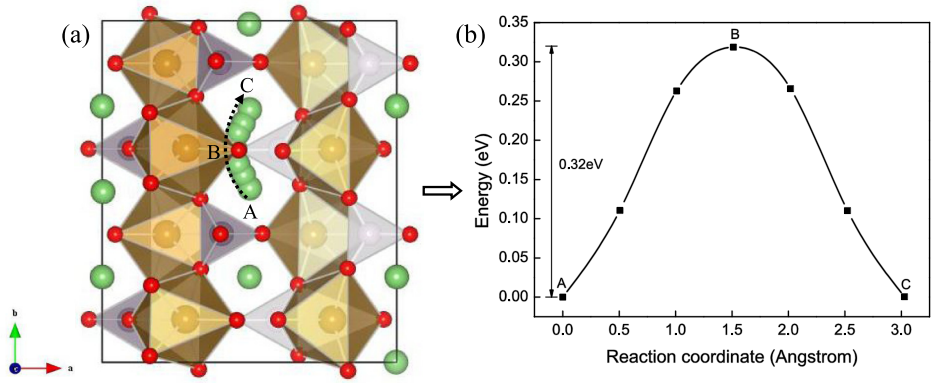

FIG. 5. Minimum energy path and activation energy for Li diffusion along the b-channel in bulk $LiFePO_4$.

suggested that, instead of thermal excitation of an electron or hole over the bandgap, the small polaron localized around a transition metal (TM) ion is likely to determine the electronic conductivity, our analysis based on the relationship between the band gap and electronic conductivity still provides valuable information on the electronic conductivity change. The result of PDOS in Fig. 2(b) reveals that the 3*d*-electrons of the Fe are the primary contributor to both the valence-band maximum (VBM) and conduction-band minimum (CBM) and the electronic states near the Fermi level (at 0 eV) result mainly from the contributions of Fe-3*d* and O-2*p* orbitals.

Fig. 3(a) shows the total DOS of the $LiFePO_4$ (010) surface within the GGA + U level. From the figure, it is found that, compared to the larger band gap of 3.58 eV for bulk $LiFePO_4$, a narrower band gap with 1.38 eV is obtained for the surface, which suggests that the plate-type nano-$LiFePO_4$ with (010) surface may exhibit better electronic conduction. From the Figs. 3(a) and 3(b), it can be seen that Fe-3*d* states are also the primary contributor to both the VBM and CBM. Analysis of the atomic PDOS on the surface region and the bulk material reveals only small changes for the Li and P atoms. The PDOS of Fe atoms at different positions varies substantially, as seen in Fig. 3(b). The PDOS of Fe atoms located at the surface differs greatly and leads to a narrower band gap.

Figs. 4(a) and 4(b) present the total DOS and PDOS of O-2*p*, S-2*p*, and Fe-3*d* of the S-$LiFePO_4$ (010) surface. From Fig. 4(a), it can be seen that new states appear in the band gap of the pure $LiFePO_4$ (010) surface after S adsorption and the band gap decreases from 1.38 eV to 0.67 eV, which might also contribute to the increased electronic conductivity. The gap states are induced by the interaction of the Fe-S bond and the hybridization of Fe-3*d* and S-2*p* leads to a narrower band gap, as shown in Fig. 4(b).

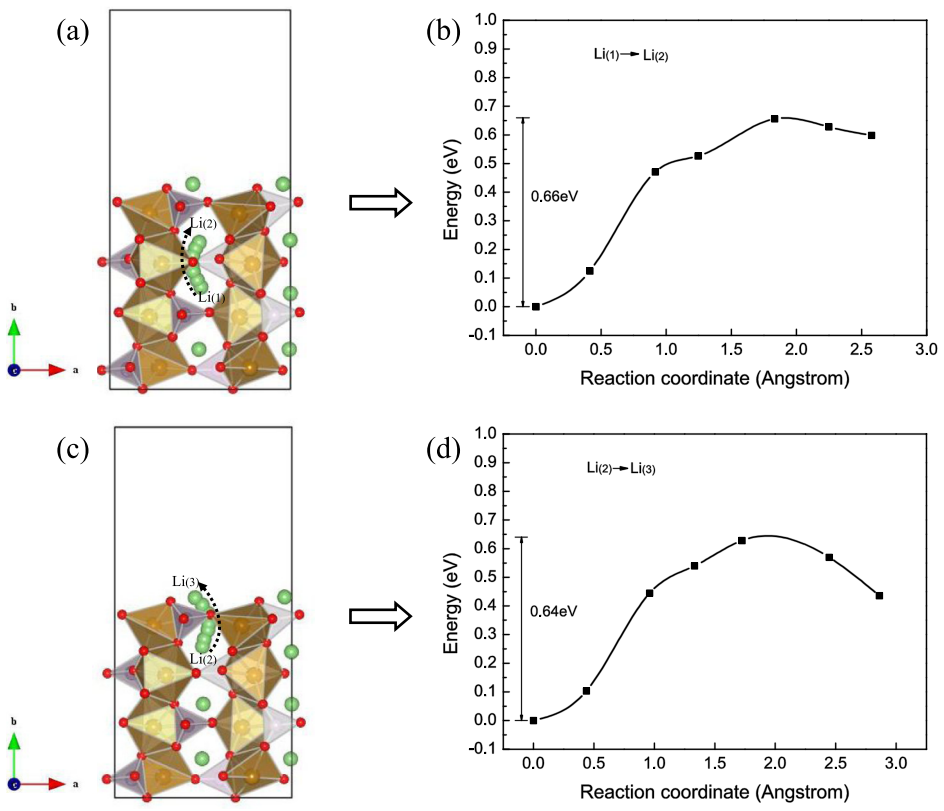

FIG. 6. Minimum energy paths and activation energies for Li diffusion along the b-channel of the pure $LiFePO_4$ (010) surface.

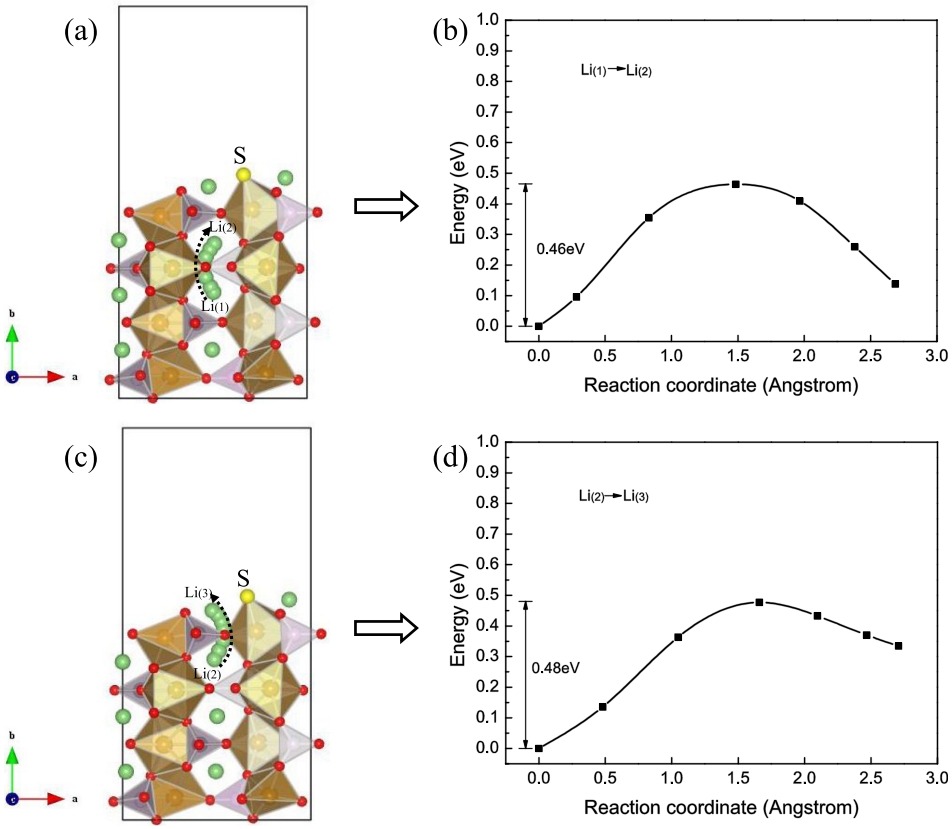

FIG. 7. Minimum energy paths and activation energies for Li diffusion along the b-channel of the S-$LiFePO_4$ (010) surface.

C. Li diffusion

Fast Li diffusion in a crystal structure of electrode materials is essential to the high-power capability of Li rechargeable batteries. In this section, NEB method has been used to calculate the activation energies and determine the minimum energy paths of Li diffusion along the b-channel. It is found that the Li-ion diffusion paths along the *b*-channel are arch-like curves, due to electrostatic repulsion between Li ion and Fe ion, as shown in Figs. 5(a), 6(a), 6(c), 7(a), and 7(c). The calculated activation energy for Li-ion diffusion in bulk $LiFePO_4$ is 0.32 eV, as shown in Fig. 5(b), which is consistent with the previously reported values with DFT + U.[19] Figs. 6(b) and 6(d) show activation energies for Li-ion interlayer diffusions from $Li_{(1)}$ site to $Li_{(2)}$ site and from $Li_{(2)}$ site to $Li_{(3)}$ site in different layers along the *b*-channel of the pure $LiFePO_4$ (010) surface. The calculated values are 0.66 eV and 0.64 eV, respectively. Activation energy for Li-ion surface diffusion is about 0.34 eV higher than that of bulk diffusion. Since Li ions should overcome both bulk and surface activation energies to diffuse along the *b*-channel, hopping through the surface barrier is likely to be a rate-limiting step for Li mobility. Therefore, the activation energy for surface diffusion must be considered for Li diffusion along the b-channel. Efforts should be made to reduce the surface diffusion barrier with proper surface modification in order to optimize rate performance.

Figs. 7(b) and 7(d) show the activation energies for Li ion diffusion along the *b*-channel of the S-$LiFePO_4$ (010) surface. The calculated values for Li ion diffusion from $Li_{(1)}$ site to $Li_{(2)}$ site and from $Li_{(2)}$ site to $Li_{(3)}$ site are 0.46 eV and 0.48 eV, respectively. Compared to the pure $LiFePO_4$ (010) surface, sulfur adsorption decreased activation energy of about 0.18 eV for Li-ion diffusion on the S-$LiFePO_4$ (010) surface, implying that the ionic conductivity would be improved obviously by sulfur surface modification. As shown in Fig. 1(c), sulfur binds directly to a surface Fe atom forming a Fe-S bond, providing full coordination of the Fe center. The electronic environment of Li^+ is close to that in the bulk $LiFePO_4$ and therefore the surface activation energies decrease. The diffusion constant can be estimated as[34]

$$D = a^2 \nu \exp(-E_{act}/k_B T), \tag{3}$$

where ν is the attempt frequency and E_{act} is the activation energy for the hop. Assuming that ν is about 10^{13} Hz, which is generally in the range of phonon frequencies, and a is approximately 3 Å, corresponding to the distance of a hop

TABLE I. The calculated band gaps, activation energies, and diffusion constants for bulk $LiFePO_4$, $LiFePO_4$ (010), and S-$LiFePO_4$ (010), respectively.

	Band gap (eV)	Activation energy (eV)	Diffusion constant (cm^2/s)
Bulk $LiFePO_4$	3.58	0.32	2.0×10^{-8}
$LiFePO_4$ (010)	1.38	0.66, 0.64	4.6×10^{-14},1.3×10^{-13}
S-$LiFePO_4$ (010)	0.67	0.46, 0.48	1.37×10^{-10},5×10^{-11}

along the [010] direction. The estimated diffusion constants are listed in Table I for various models being considered. The diffusion constant of the S-$LiFePO_4$ (010) surface can be approximated to be 10^{-11} (cm^2/s) at room temperature and Li diffusivity in the S-$LiFePO_4$ (010) surface is expected to be faster by three orders of magnitude than that of the pure $LiFePO_4$ (010) surface. Therefore, it can be expected that sulfur adsorption on the $LiFePO_4$ (010) surface will improve Li ion transport properties well.

IV. CONCLUSIONS

In conclusion, we have investigated the electronic and Li-ion diffusion properties of the $LiFePO_4$ (010) surface modified by sulfur with first-principles calculations under the DFT + U framework. It is found that the sulfur adsorption on the $LiFePO_4$ (010) surface is energetically favored. A much narrower band gap of the S-$LiFePO_4$ (010) surface is predicted. The activation energy for Li diffusion on the S-$LiFePO_4$ (010) surface is predicted to be lower than that of the pure $LiFePO_4$ (010) surface with the nudged elastic band method. The estimated Li diffusion coefficient of the sulfur surface-modified $LiFePO_4$ is approximated to be 10^{-11} (cm^2/s) at room temperature, which is about 10^3 times larger than that of the pure $LiFePO_4$ (010) surface. The above results mean that the sulfur surface-modified $LiFePO_4$ will exhibit higher electronic and ionic conductivity, which gives rise to the enhanced electrochemical performance.

ACKNOWLEDGMENTS

This work was supported by the National Natural Science Foundation of China (No. 11204038), the National Key Project for Basic Research of China (No. 2011CBA-00200), Educational Department of Fujian Province, China (No. JA12376).

[1]L. Dimesso, C. Spanheimer, W. Jaegermann, Y. Zhang, and A. L. Yarin, J. Appl. Phys. **111**, 064307 (2012).
[2]B. L. Ellis, K. T. Lee, and L. F. Nazar, Chem. Mater. **22**, 691–714 (2010).
[3]J. Lee, W. Zhou, J. C. Idrobo, S. J. Pennycook, and S. T. Pantelides, Phys. Rev. Lett. **107**, 085507 (2011).
[4]P. P. Prosini, M. Lisi, D. Zane, and M. Pasquali, Solid State Ionics **148**, 45–51 (2002).
[5]J. Barker, M. Y. Saidi, and J. L. Swoyer, Electrochem. Solid-State Lett. **6**, A53–A55 (2003).
[6]Z. H. Wang, L. X. Yuan, M. Wu, D. Sun, and Y. H. Huang, Electrochim. Acta **56**, 8477–8483 (2011).
[7]I. Bilecka, A. Hintennach, M. D. Rossell, D. Xie, P. Novak, and M. Niederberger, J. Mater. Chem. **21**, 5881–5890 (2011).
[8]C. Delmas, M. Maccario, L. Croguennec, F. L. Cras, and F. Weill, Nat. Mater. **7**, 665–671 (2008).
[9]J. Lee, S. J. Pennycook, and S. T. Pantelides, Appl. Phys. Lett. **101**, 033901 (2012).
[10]M. Wang, W. Zhang, Y. H. Liu, Y. Yang, C. S. Wang, and Y. Wang, Appl. Phys. Lett. **104**, 171604 (2014).
[11]Y. B. Lin, Y. Lin, T. Zhou, G. Y. Zhao, Y. D. Huang, and Z. G. Huang, J. Power Sources **226**, 20–26 (2013).
[12]N. Ravet, Y. Chouinard, J. F. Magnan, S. Besner, M. Gauthier, and M. Armand, J. Power Sources **97–98**, 503–507 (2001).
[13]K. S. Park, P. H. Xiao, S. Y. Kim, A. Dylla, Y. M. Choi, G. Henkelman, K. J. Stevenson, and J. B. Goodenough, Chem. Mater. **24**, 3212–3218 (2012).
[14]D. Morgan, A. Van der Ven, and G. Ceder, Electrochem. Solid-State Lett. **7**, A30–A32 (2004).
[15]C. Y. Ouyang, S. Q. Shi, Z. X. Wang, X. J. Huang, and L. Q. Chen, Phys. Rev. B **69**, 104303 (2004).
[16]S. Nishimura, G. Kobayashi, K. Ohoyama, R. Kanno, M. Yashima, and A. Yamada, Nat. Mater. **7**, 707–711 (2008).
[17]L. Wang, F. Zhou, Y. S. Meng, and G. Ceder, Phys. Rev. B **76**, 165435 (2007).
[18]R. G. Mei, X. R. Song, Y. F. Yang, Z. G. An, and J. J. Zhang, RSC Adv. **4**, 5746–5752 (2014).
[19]G. K. P. Dathar, D. Sheppard, K. J. Stevenson, and G. Henkelman, Chem. Mater. **23**, 4032–4037 (2011).
[20]J. P. Perdew, J. A. Chevary, S. H. Vosko, K. A. Jackson, M. R. Pederson, D. J. Singh, and C. Fiolhais, Phys. Rev. B **46**, 6671 (1992).
[21]G. Kresse and J. Furthmüller, Phys. Rev. B **54**, 11169 (1996).
[22]G. Kresse and J. Furthmüller, Comput. Mater. Sci. **6**, 15–50 (1996).
[23]S. L. Dudarev, G. A. Botton, S. Y. Savrasov, C. J. Humphreys, and A. P. Sutton, Phys. Rev. B **57**, 1505 (1998).
[24]F. Zhou, M. Cococcioni, C. A. Marianetti, D. Morgan, and G. Ceder, Phys. Rev. B **70**, 235121 (2004).
[25]S. P. Ong, V. L. Chevrier, and G. Ceder, Phys. Rev. B **83**, 075112 (2011).
[26]G. G. Xu, Q. Y. Wu, Z. G. Chen, Z. G. Huang, and Y. P. Feng, J. Appl. Phys. **106**, 043708 (2009).
[27]G. Henkelman, B. P. Uberuaga, and H. Jónsson, J. Chem. Phys. **113**, 9901 (2000).
[28]S. Q. Shi, L. J. Liu, C. Y. Ouyang, D. S. Wang, Z. X. Wang, L. Q. Chen, and X. J. Huang, Phys. Rev. B **68**, 195108 (2003).
[29]T. Maxisch and G. Ceder, Phys. Rev. B **73**, 174112 (2006).
[30]P. X. Zhang, D. Y. Zhang, L. Huang, Q. Wei, M. C. Lin, and X. Z. Ren, J. Alloys Compd. **540**, 121–126 (2012).
[31]K. Hoang and M. Johannes, Chem. Mater. **23**, 3003–3013 (2011).
[32]F. Zhou, K. Kang, T. Maxisch, G. Ceder, and D. Morgan, Solid State Commun. **132**, 181–186 (2004).
[33]K. Zaghib, A. Mauger, J. B. Goodenough, F. Gendron, and C. M. Julien, Chem. Mater. **19**, 3740–3747 (2007).
[34]D. H. Seo, Y. U. Park, S. W. Kim, I. Park, R. A. Shakoor, and K. Kang, Phys. Rev. B **83**, 205127 (2011).